Available online at http://scik.org
J. Math. Comput. Sci. 2022, 12:55
https://doi.org/10.28919/jmcs/6942
ISSN: 1927-5307

AN ALTERNATIVE METHOD FOR INVESTIGATING THE EFFECT OF SQUEEZING FLOW OF A CASSON FLUID BETWEEN PARALLEL WALLS ON MAGNETIC FIELD

SAHEED ALAO[1], RASAQ ADEKOLA ODERINU[1,*], EMMANUEL IDOWU AKINOLA[2], OLUSOLA EMMANUEL OPALEYE[1]

[1]Department of Pure and Applied Mathematics, Ladoke Akintola University of Technology, Ogbomoso, Nigeria
[2]Mathematics Programme, Bowen University Iwo, Nigeria

Abstract. In this article, the Magnetohydrodynamics (MHD) Casson fluid between parallel plate is numerically investigated. The nonlinear ordinary differential equation arising from the governing equations was numerically analyzed using collocation method of weighted residual. The efficiency of the method was measured by comparing the solutions obtained with the literatures. The compared results were found to be in excellent agreement. Flow behavior under the influence of physical variables (Squeeze number S, Casson fluid γ and Magnet number M) were presented in tabular and graphical form.

Keywords: magnetohydrodynamics; weighted residual method; magnetic number; squeeze number; Casson fluid.

2010 AMS Subject Classification: 33F05, 34K28, 35A35, 65L10.

1. INTRODUCTION

Several researches of non-Newtonian squeezing flow between parallel plates or walls that have applications in technical, mechanical and biological systems have been studied. The unsteady squeezing flow of a viscous fluid between parallel walls in motion normal to it own

*Corresponding author
E-mail address: raoderinu@lautech.edu.ng
Received October 28, 2021

surfaces is of high importance in hydrodynamical tools such as Casson fluid. Due to this industrial importance, squeezing flow between parallel walls has become one of the most relevant research field in fluid studies. The foremost research and formulation on squeezing flow can be traced to Stefan[1], who presented fundamental idea of these type of flows under lubrication. Scholars over the years have shown interests in understanding and analyzing squeezing flow, Sobamowo et al.[2] studied MHD squeezing flow analysis of nanofluid under effect of slip boundary conditions, the authors utilized variation of parameter method to analytically study the effects of fluid properties, magnetic field and slip variables. Abdul-Sattar et al.[3] established an algorithm for investigating the effect of squeezing flow of a Casson fluid between parallel walls on magnetic field. The authors demonstrated the effectiveness of the algorithm by proving the convergence of the solution obtained in series form. Naveed et. al.[4] suggested that magnetic field can be utilized as a control parameter in numerous flow as it stabilizes the flow conduct, flow conduct under the physical variables such as squeeze number and Casson fluid were taken into consideration. Hayat et. al.[5] presented an exact solution of MHD squeezing flow of couple stress nanomaterial along two parallel surfaces and the detail effect of velocity, temperature and concentration field was studied via homotopic approach. The MHD squeezing flow linking two parallel disks under the effect of sunction and injection was examined by Domairry and Aziz[6] using homotopy method. Domairry and Hatami [7] studied the unsteady squeezing flow of CU-water nano fluid between parallel surfaces via differential transform method while Sheikholeslami and Ganji[8] investigated the squeezing flow of CU-water nano fluid between parallel surfaces. Mostafa et al. [9] investigated the existence and uniqueness of solution for squeezing nanofluid flow using Green-Picard's iteration as the pioneer study. The nonlinear radiation effects on squeezing flow of a Casson fluid between parallel disk was examined Mohyud-Din and Khan [10]. In this article, our interest is to show the effectiveness and accuracy of weighted residual method (WRM) to solve Casson squeeze flow between parallel walls and the residual is minimized by collocating the boundary of the problem.

2. Governing Equation

The equation governing the Casson fluid squeezing flow between parallel walls was derived by Abdul-Sattar et. al.[3] and Naveed et. al.[4] as

$$(1+\frac{1}{\gamma})F'''' - S(\eta F'''(\eta)+3F''(\eta)+F'(\eta)F''(\eta)-F(\eta)F'''(\eta)) - M^2F''(\eta) = 0 \tag{1}$$

with boundary condition

$$F(0)=0,\ F''(0)=0\ F(1)=1\ F'(1)=0 \tag{2}$$

where γ= Casson fluid variable, S =Squeeze number and M=Magnetic number

3. Method of Solution

Following the stepwise procedure of weighted residual method as discussed in [11-13], the choice of trial function is in the form

$$F=\sum_{i=0}^{N} a_i\eta^i \tag{3}$$

where N chosen as 13 is a whole number and a_i are unknown constants to be solved for. Based on the procedure, the trial function need to satisfy all the given boundary conditions, therefore, the boundary condition in equation (2) is forced on equation(3) to obtain system of equations

(4)

$$a_0 = 0$$

$$2a_2 = 0$$

$$a_0+a_1+a_2+a_3+a_4+a_5+a_6+a_7+a_8+a_9+a_{10}+a_{11}+a_{12}+a_{13}=1$$

$$a_1+2a_2+3a_3+4a_4+5a_5+6a_6+7a_7+8a_8+9a_9+10a_{10}+11a_{11}+12a_{12}+13a_{13}=0$$

The residual equation is derived by substituting the trial function into equation (1) as

(5)

$$R(\eta) = -13.8138a_3\eta - 27.6276a_4\eta^2 - 46.0460a_5\eta^3 - 69.0690a_6\eta^4 - 96.6966a_7\eta^5 - 128.9288a_8\eta^6 - 165.7656a_9\eta^7 - 207.2070a_{10}\eta^8 - 253.2530a_{11}\eta^9 - 303.9036a_{12}\eta^{10} - 359.1588a_{13}\eta^{11}360\eta^2a_6 + 120\eta a_5 + 840a_7\eta^3 + 1680a_8\eta^4 + 3024a_9\eta^5 + 5040a_{10}\eta^6 + 7920a_{11}\eta^7 + 11880a_{12}\eta^8 + 17160a_{13}\eta^9 - 0.4341\eta(6a_3 + 24a_4\eta + 60a_5\eta^2 + 120a_6\eta^3 + 210a_7\eta^4 + 336a_8\eta^5 + 504a_9\eta^6 + 720a_{10}\eta^7 + 990a_{11}\eta^8 + 1320a_{12}\eta^9 + 1716a_{13}\eta^{10}) - 4.6046a_2 + 24a_4 + (.4341(a_0 + a_1\eta + a_2\eta^2 + a_3\eta^3 + a_4\eta^4 + a_5\eta^5 + a_6\eta^6 + a_7\eta^7 + a_8\eta^8 + a_9\eta^9 + a_{10}\eta^{10} + a_{11}\eta^{11} + a_{12}\eta^{12} + a_{13}\eta^{13}))(6a_3 + 24a_4\eta + 60a_5\eta^2 + 120a_6\eta^3 + 210a_7\eta^4 + 336a_8\eta^5 + 504a_9\eta^6 + 720a_{10}\eta^7 + 990a_{11}\eta^8 + 1320a_{12}\eta^9 + 1716a_{13}\eta^{10}) - (0.4341(a_1 + 2a_2\eta + 3a_3\eta^2 + 4a_4eta^3 + 5a_5\eta^4 + 6a_6\eta^5 + 7a_7\eta^6 + 8a_8\eta^7 + 9a_9\eta^8 + 10a_{10}\eta^9 + 11a_{11}\eta^{10} + 12a_{12}\eta^{11} + 13a_{13}\eta^{12}))(2a_2 + 6a_3\eta + 12a_4\eta^2 + 20a_5\eta^3 + 30a_6\eta^4 + 42a_7\eta^5 + 56a_8\eta^6 + 72a_9\eta^7 + 90a_{10}\eta^8 + 110a_{11}\eta^9 + 132a_{12}\eta^{10} + 156a_{13}\eta^{11})$$

The residual function is then minimized using collocation in the range [0, 1] and as a result, system of equations are obtained. The obtained systems of equation along with equation(4) were solved using Maple 18 mathematical software simultaneously to get the unknown constants.

(6)

$$a_0 = 0, a_1 = 1.442922969, a_2 = 0, a_3 = -0.3878399355, a_4 = 0, a_5 = -0.05306424376$$
$$, a_6 = -1.508638757 \times 10^{-7}, a_7 = -0.002037871902, a_8 = -0.2175899242 \times 10^{-5},$$
$$a_9 = 0.1952645010 \times 10^{4}, a_{10} = -0.5747973677 \times 10^{-5}, a_{11} = 0.9296473413 \times 10^{-5},$$
$$a_{12} = -0.2607241628 \times 10^{-5}, a_{13} = 9.415078602 \times 10^{-7}$$

The constants are then substituted into equation(3) to obtain the required solution

(7)

$$F(\eta) = 1.442922969\eta - 0.3878399355\eta^3 - 0.05306424376\eta^5 - 1.508638757 \times 10^{-7}\eta^6$$
$$-0.002037871902\eta^7 - 0.2175899242 \times 10^{-5}\eta^8 + 0.1952645010 \times 10^{-4}\eta^9$$
$$-0.5747973677 \times 10^{-5}\eta^{10} + 0.9296473413 \times 10^{-5}\eta^{11} - 0.2607241628 \times 10^{-5}\eta^{12}$$
$$+9.415078602 \times 10^{-7}\eta^{13}.$$

for $S = 0.4341, \gamma = \infty, M = 1$

4. RESULTS AND DISCUSSIONS

In order to present the validity of the WRM solutions, the effects of S, γ and M on the axial $F(\eta)$ and radial $F'(\eta)$ velocities are presented. Figures 1 and 2 show the influence of positive values of S on $F(\eta)$ and $F'(\eta)$. Figure 1 shows that an increase in S leads to decrease in $F(\eta)$ while figure 2 shows that as S increases the curve $F'(\eta)$ decreases and increase at $0.5 < \eta \leq 1$. Figures 3 and 4 show the influence of negative values of S on $F(\eta)$ and $F'(\eta)$. Decrease in S increases $F(\eta)$ as shown in figure 3 while as S increases, a significant increase in $F'(\eta)$ is noticed at $\eta \leq 0.5$. Moreover, there is a rapid decrease at $0.5 < \eta \leq 1$ as displayed in figure 4. In Figures 5 and 6, the influence of varying M on $F(\eta)$ and $F'(\eta)$ are presented for positive S. As M increases, there is decrease in axial velocity as displayed in figure 5. In figure 6, variation of M (increase) leads to decreasing $F'(\eta)$ at $\eta < 0.5$ and at $0.5 < \eta \leq 1$, $F'(\eta)$ increases. Figures 7 and 8, depict the effects of varying M on $F(\eta)$ and $F'(\eta)$ for negative value S. As M increases, there is decrease in axial velocity as in figure 7. Figure 8, shows that increase in M decreases $F(\eta)$ while as M increases $F'(\eta)$ decreases until $\eta < 0.5$ and a rise in $F'(\eta)$ is noticed between $0.5 < \eta \leq 1$. Figures 9-12 are presented to study the effects of γ on $F(\eta)$ and $F'(\eta)$ for both negative and positive values of S. It can be noticed that increase inγ leads to decrease of $F(\eta)$ and also increase in γ leads to decrease of $F'(\eta)$ until otherwise at $0.5 < \eta \leq 1$ as shown in figures 9 and 10. For $S < 0$, it was observed from figures 11 and 12 respectively that increasing γ causes increase in $F(\eta)$, $F'(\eta)$ and $F'(\eta)$ decreases at $0.5 < \eta \leq 1$ as presented in figure 12. Table 1 shows the approximate values of skin friction coefficient and it can be observed that increase in all the variables leads to an increasing of magnitude of the skin friction coefficient and comparison with existing methods in literature(Novel Algorithm and Variation of parameters method(VPM)) are presented to show the accuracy of the method. while Table 2 presents the obtained solution in comparison with Wang(1976), RK-4 and VPM. Table 3 shows the comparison between the obtained results along with VPM and Novel algorithm. It was observed that the solution agrees with these methods. Tables 4 and 5 represent the comparison between the existing solutions and WRM for axial and radial velocities taking squeeze number $S = 1$ and $S = -1$ respectively while the numerical values of unknown constants $F'(0)$ and $F'''(0)$ in comparison with VPM are presented in Table 6.

TABLE 1. Comparing the results of skin friction coefficient $(1+\frac{1}{\gamma})F''(1)$

S	γ	M	WRM	Novel Algorithm[3]	VPM[4]
-5	0.4	1	-6.2987081	-6.3949610	-6.2987080
-3	0.4	1	-8.3207271	-8.3207270	-8.3207271
-1	0.4	1	-9.9703768	-9.9705750	-9.9703760
1	0.4	1	-11.376241	-11.375837	-11.376240
3	0.4	1	-12.618670	-12.604612	-12.6100669
5	0.4	1	-13.718095	-13.697927	-13.718095
-3	0.1	1	-30.991005	-30.991843	-30.991005
-3	0.3	1	-10.873387	-10.851771	-10.873387
-3	0.5	1	-6.7715490	-6.7896240	-6.7715490
3	0.1	1	-35.260197	-35.260196	-35.260196
3	0.3	1	-15.149577	-15.145259	-15.149577
3	0.5	1	-11.078736	-11.071084	-11.078736
3	0.4	2	-9.0381967	-9.0435300	-9.0381960
-3	0.4	4	-11.531984	-11.532951	-11.531981
-3	0.4	6	-14.819321	-14.819321	-14.819321
3	0.4	2	-13.1015722	-13.092241	-13.101572
3	0.4	4	-14.908219	-14.908219	-14.908219
3	0.4	6	-17.501185	-17.471534	-17.501183

TABLE 2. Comparison of WRM with existing results as $M = 0$ and $\gamma \to \infty$ for $F''(1)$.

S	WRM	WANG(1976)[4]	RK-4[4]	VPM[4]
-0.9780	-2.1915	-2.2350	-2.1915	-2.1915
-0.4977	-2.6193	-2.6272	-2.6193	-2.6193
-0.09998	-2.9277	-2.9279	-2.9277	-2.9277
0.0000	-3.0000	-3.0000	-3.0000	-3.0000
0.09403	-3.0664	-3.0665	-3.0663	-3.0663
0.4341	-3.2943	-3.2969	-3.2943	-3.2943
1.1224	-3.7080	-3.7140	-3.7080	-3.7080

TABLE 3. Comparison of $F(\eta)$ for $M = 1$ and $\gamma = 0.4$

	S=5			S=-5		
η	WRM	Novel Algoritm[3]	VPM[4]	WRM	Novel Algorithm[3]	VPM[4]
0.1	0.139081	0.139103	0.139081	0.166840	0.166665	0.166839
0.2	0.276358	0.276402	0.276358	0.328445	0.328112	0.328444
0.3	0.409918	0.409981	0.409918	0.479862	0.479402	0.479861
0.4	0.537629	0.537705	0.537628	0.616686	0.616144	0.616685
0.5	0.657014	0.657098	0.657014	0.735287	0.734719	0.735286
0.6	0.765125	0.765208	0.765125	0.832994	0.832465	0.832992
0.7	0.858383	0.858455	0.858383	0.908218	0.907792	0.908218
0.8	0.932409	0.932458	0.932408	0.960506	0.960237	0.960506
0.9	0.981820	0.981839	0.981819	0.990529	0.990434	0.990529

TABLE 4. Comparison between WRM with existing results for $M = 1$, $\gamma = 0.2$, $S = 1$.

	$F(\eta)$			$F'(\eta)$		
η	WRM	Novel Algoritm[3]	RK-4[3]	WRM	Novel Algorithm[3]	RK-4[3]
0.1	0.147656	0.147656	0.147656	1.467311	1.467313	1.467313
0.2	0.292534	0.292534	0.292534	1.425574	1.425575	1.425575
0.3	0.431831	0.431831	0.431832	1.355628	1.355629	1.355629
0.4	0.562700	0.562701	0.562701	1.256897	1.256898	1.256899
0.5	0.682225	0.682225	0.682226	1.128583	1.128583	1.128583
0.6	0.787397	0.787397	0.787398	0.969660	0.969661	0.969661
0.7	0.875095	0.875096	0.875097	0.778890	0.778889	0.778881
0.8	0.942065	0.942065	0.942067	0.554822	0.554821	0.554821
0.9	0.984895	0.984897	0.984895	0.295805	0.295804	0.295804

TABLE 5. Comparison between WRM with existing results for $M = 1$, $\gamma = 0.2$, $S = -1$.

	$F(\eta)$			$F'(\eta)$		
η	WRM	Novel Algoritm[3]	RK-4[3]	WRM	Novel Algorithm[3]	RK-4[3]
0.1	0.150638	0.150638	0.150638	1.495907	1.495907	1.495907
0.2	0.298136	0.298136	0.298136	1.448847	1.448847	1.448847
0.3	0.439361	0.439360	0.439361	1.370673	1.370673	1.370673
0.4	0.571247	0.571246	0.571246	1.261767	1.261767	1.261767
0.5	0.690717	0.690716	0.690716	1.122651	1.122650	1.122650
0.6	0.794791	0.794791	0.794790	0.953971	0.953971	0.953971
0.7	0.880551	0.880550	0.880541	0.756487	0.756487	0.756487
0.8	0.945156	0.945156	0.945156	0.531046	0.531047	0.531047
0.9	0.985856	0.985858	0.985876	0.278565	0.278565	0.278566

TABLE 6. Comparison between WRM with existing result for convergence of $F'(0)$ and $F'''(0)$ as $M = 1$, $\gamma = 0.2$.

Method	$F'(0)$	$F'''(0)$	$F'(0)$	$F'''(0)$
WRM	1.481185453	-2.772858804	1.511619702	-3.143841600
Abdul-Sattar and Abeer [3]	1.481186659	-2.772867578	1.511619152	-3.143837395

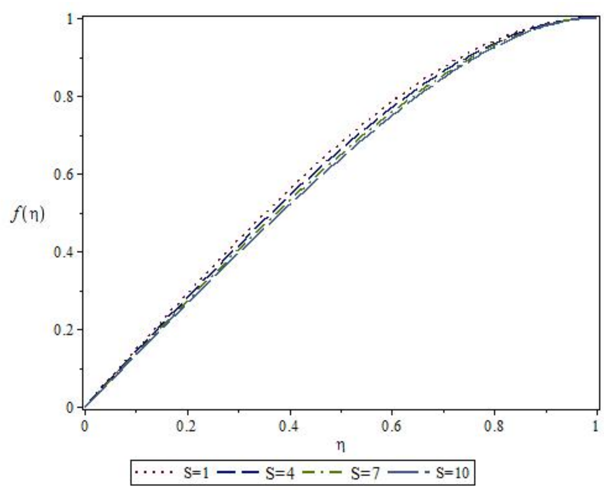

FIGURE 1. Variants of positive values of S on $F(\eta)$ when $M = 1$, $\gamma = 0.4$.

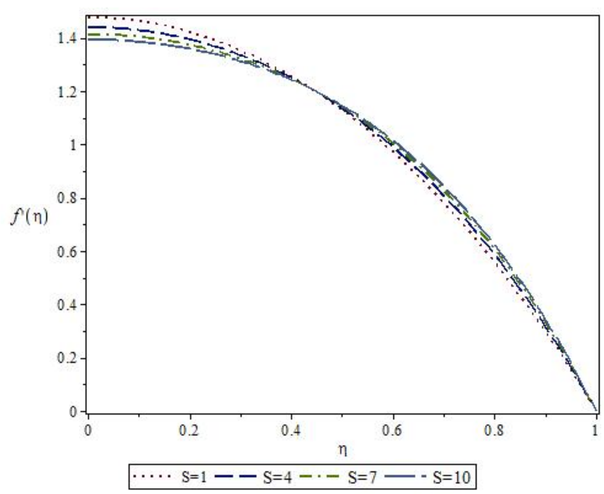

FIGURE 2. Variants of positive values of S on $F'(\eta)$ when $M = 1$, $\gamma = 0.4$.

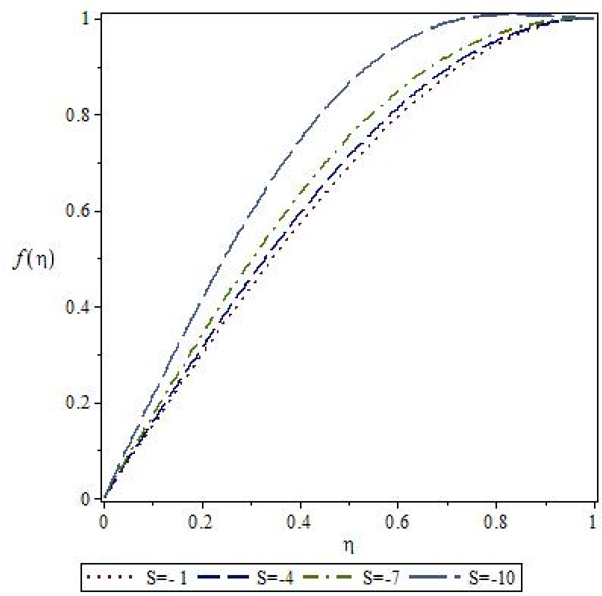

FIGURE 3. Variants of negative values of S on $F(\eta)$ when $M = 1$, $\gamma = 0.4$.

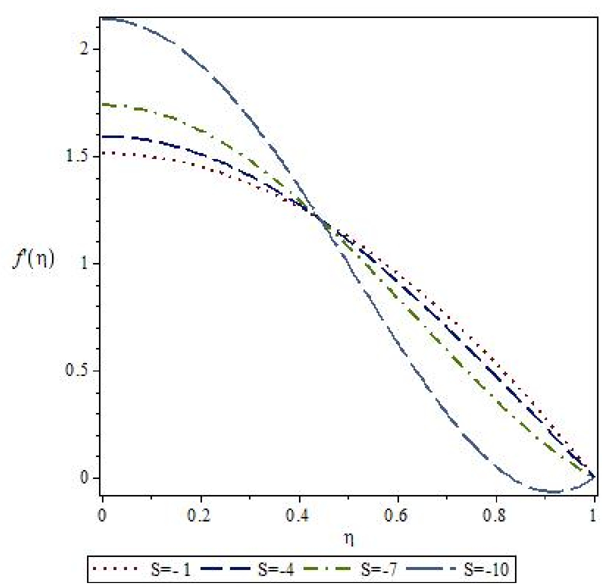

FIGURE 4. Variants of negative values of S on $F'(\eta)$ when $M = 1$, $\gamma = 0.4$.

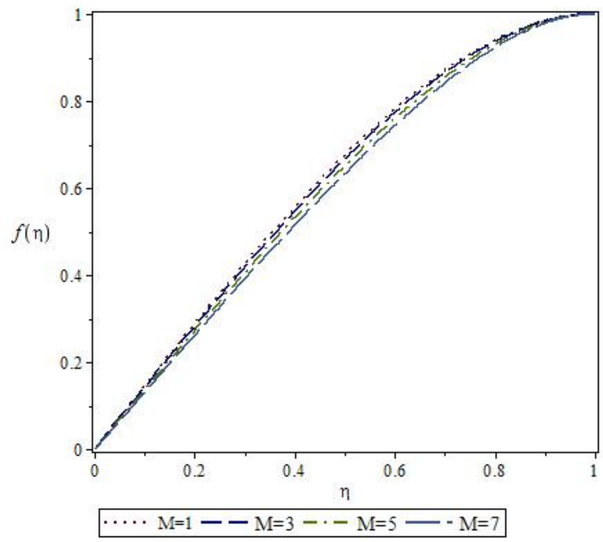

FIGURE 5. Variants of M on $F(\eta)$ when $S=3$, $\gamma=0.3$.

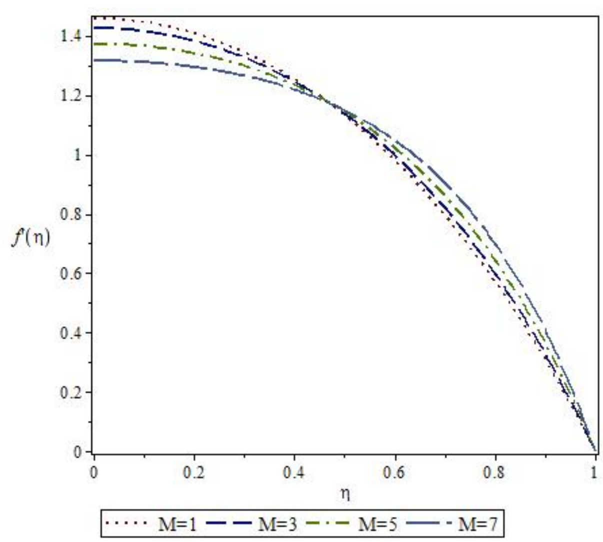

FIGURE 6. Variants of M on $F'(\eta)$ when $S=3$, $\gamma=0.3$.

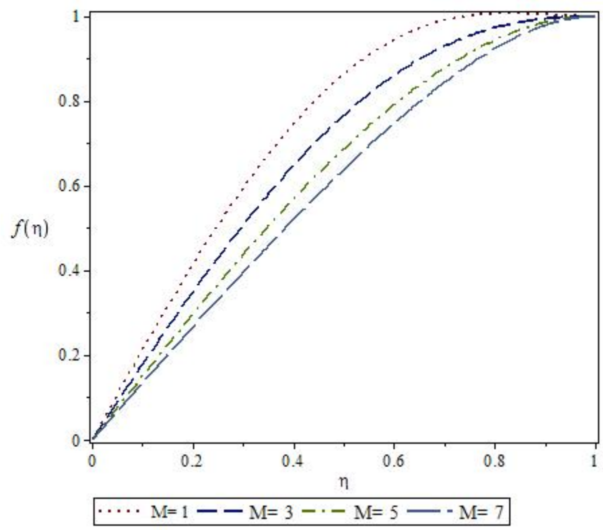

FIGURE 7. Variants of M on $F(\eta)$ when $S=-10$, $\gamma=0.4$.

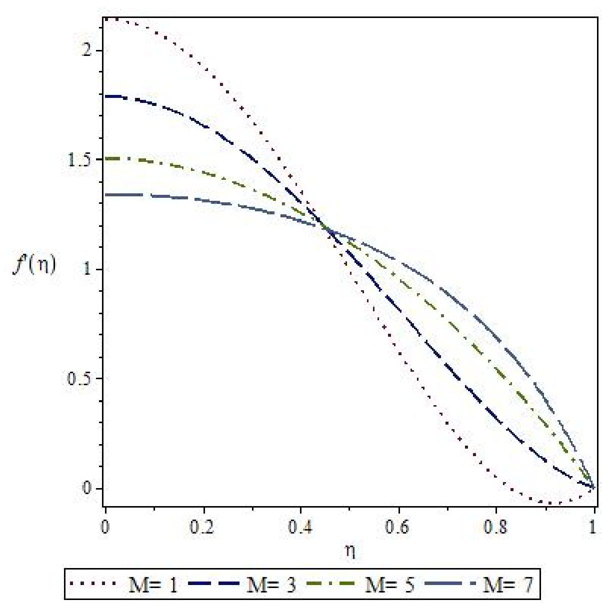

FIGURE 8. Variants of M on $F'(\eta)$ when $S=-10$, $\gamma=0.4$.

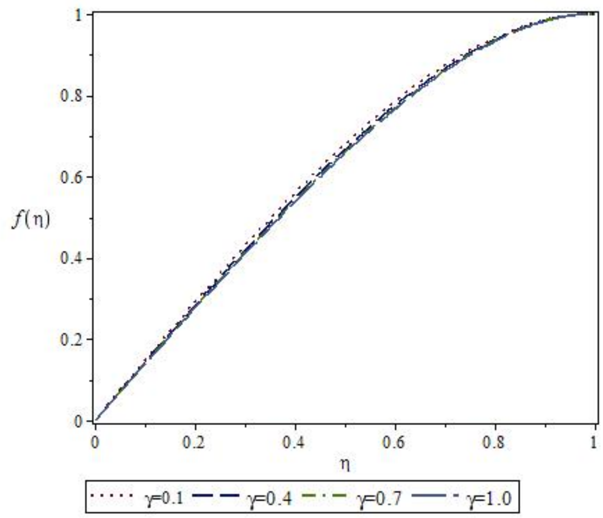

FIGURE 9. Variants of γ on $F(\eta)$ when $S=4$, $M=2$.

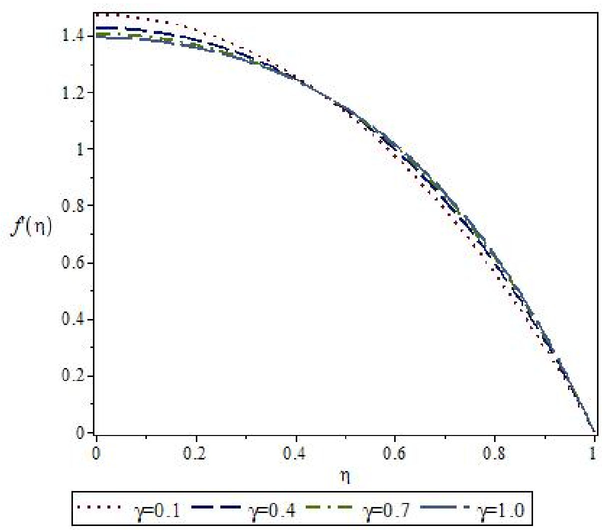

FIGURE 10. Variants of γ on $F'(\eta)$ when $S=4$, $M=2$.

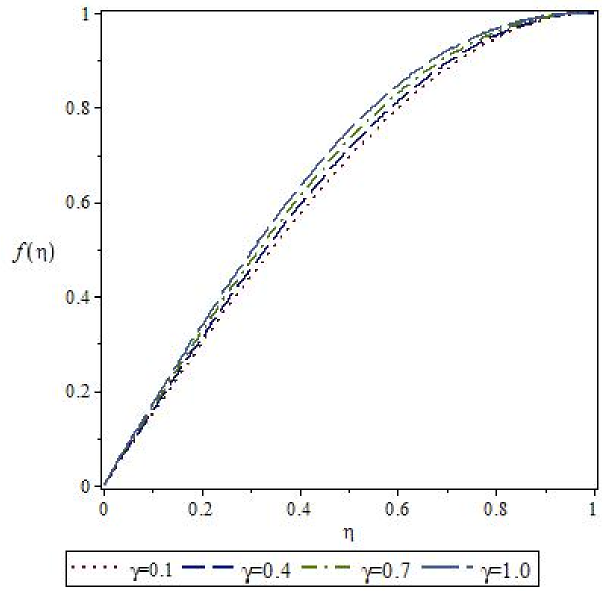

FIGURE 11. Variants of γ on $F(\eta)$ when $S = -5, M = 2$.

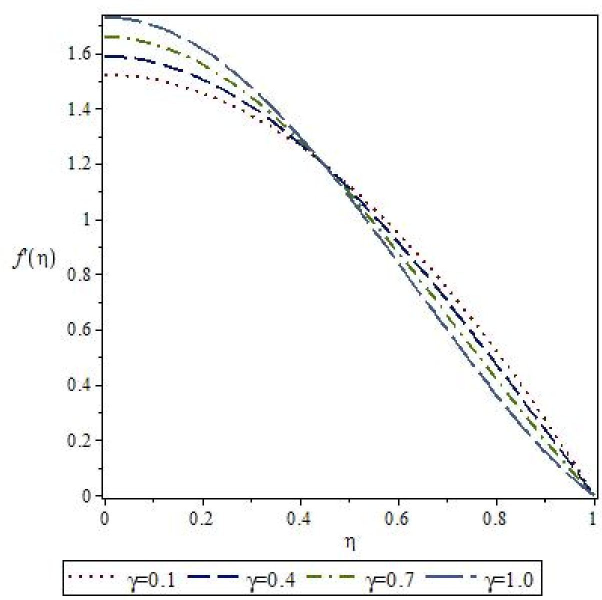

FIGURE 12. Variants of γ on $F'(\eta)$ when $S = -5, M = 2$.

5. Conclusion

In this article, the numerical solution of squeezing MHD Casson flow have been investigated using WRM as an alternative to existing methods in literature. The method presents solution in form of polynomial which avoids discretization error. Flexibility of the method in terms of trial function also allows improvement on the accuracy of the solution.

Conflict of Interests

The authors declare that there is no conflict of interests.

References

[1] M.J. Stefan, Versuch Uber die scheinbare adhesion, Sitzungsber. Akad. Wissen. Wien. Math. Naturwissen. 69 (1874), 713-721.

[2] M.G. Sobamowo, L.O. Jayesimi and M.A. Waheed, Magnetohydrodynamic squeezing flow analysis of nanofluid under the effect of slip boundary conditions using variation of parameter method, Karbala Int. J. Modern Sci. 4 (2018), 107-118.

[3] J.A. Abdul-Sattar, Al-Saif, M.J. Abeer, A novel algorithm for studying the effect of squeezing flow of a casson fluid between parallel plates on magnetic field, Journal of Applied Mathematics. 2019 (2019), 3679373.

[4] N. Ahmed, U. Khan, S. I. Khan, S. Bano, and S. T. Mohyud-Din, Effects on magnetic field in squeezing flow of a Casson fluid between parallel plates, J. King Saud Univ.-Sci. 29 (2017), 119-125.

[5] T. Hayat, R. Sajjad, A. Alsaedi, T Muhammad, and R. Ellahi, On squeezed flow of couple stress nanofluid between two parallel plates, Results Phys. 7 (2017), 553-561.

[6] G. Domairry and A. Aziz, Approximate analysis of MHD squeeze flow between two parallel disks with suction or injection by homotopy perturbation method, Math. Prob. Eng. 2019 (2009), 603916.

[7] G. Domairry and H. Hatami, Squeezing Cu-water nanofluid flow analysis between parallel plates by DTM-Pade Method. J. Mol. Liq. 193 (2014), 37-44.

[8] M. Sheikholeslami and D.D. Ganji, Heat transfer of Cu-water nanofluid flow between parallel plates, Powder Technol. 235 (2013), 873-879.

[9] E. Mostafa, H.M. Hamed and D.D. Ganji, On the existence and uniqueness of solution for squeezing nanofluid flow problem and Green-Picard's iteration, Int. J. Numer. Methods Heat Fluid Flow, 31 (2021), 2986-3008.

[10] S. T. Mohyud-Din and S. I. Khan, Nonlinear radiation effects on squeezing flow of a Casson fluid between parallel disks, Aerospace Sci. Technol. 48 (2016), 186-192.

[11] R.A. Oderinu and Y.A.S. Aregbesola, Using Laguerre's quadrature in the weighted residual method for problems with semi-infinite domain, Int. J. Pure Appl. Math. 75 (2012), 76-82.

[12] S.O. Salawu and S.S. Okoya, On criticality for a branched-chain thermal reactive-diffusion in a cylinder, Combust. Sci. Technol. 192 (2020), 1-16.

[13] S.O. Salawu, R.A. Oderinu, and A.D. Ohaegbue, Current density and thermodynamic analysis of energy optimization for double exothermic reaction of magneto-Oldroyd 8-constant material, J. King Saud Univ.-Sci. 33 (2021), 101374.